

UNCLASSIFIED

AD NUMBER

ADB015616

LIMITATION CHANGES

TO:

Approved for public release; distribution is unlimited.

FROM:

Distribution authorized to U.S. Gov't. agencies only; Test and Evaluation; 28 MAY 1976. Other requests shall be referred to Rome Air Development Center, Griffiss AFB, NY.

AUTHORITY

RADC ltr 23 Oct 1978

THIS PAGE IS UNCLASSIFIED

THIS REPORT HAS BEEN DELIMITED
AND CLEARED FOR PUBLIC RELEASE
UNDER DOD DIRECTIVE 5200.20 AND
NO RESTRICTIONS ARE IMPOSED UPON
ITS USE AND DISCLOSURE.

DISTRIBUTION STATEMENT A

APPROVED FOR PUBLIC RELEASE;
DISTRIBUTION UNLIMITED.

RADC-TR-76-194 ✓
IN-HOUSE REPORT
JUNE 1976



Experimental Simulated Plasma Results on Base-Mounted Antennas

NICHOLAS V. KARAS
JOHN D. ANTONUCCI

AD B 015616

Distribution limited to U.S. Government agencies only;
(Test and Evaluation of Commercial Products or Military
Hardware); (28 May 1976). Other requests for this
document must be referred to RADC/ETEP, Hanscom
AFB, Massachusetts 01731.

DDC
RECEIVED
DEC 20 1976
A

ROME AIR DEVELOPMENT CENTER
AIR FORCE SYSTEMS COMMAND
GRIFFISS AIR FORCE BASE, NEW YORK 13441

AW NO. _____
DDC FILE COPY Good. Fe.

Z

(1) J.

This technical report has been reviewed and approved for publication.

APPROVED: *Walter Rotman*
WALTER ROTMAN
Project Engineer

APPROVED: *Carlyle J. Sletten*
CARLYLE J. SLETTEN
Chief, Electromagnetic Sciences Division

REVISIONS	
NO.	DESCRIPTION
1	Initial Review
2	Final Review
3	Final Review
4	Final Review
5	Final Review
6	Final Review
7	Final Review
8	Final Review
9	Final Review
10	Final Review
11	Final Review
12	Final Review
13	Final Review
14	Final Review
15	Final Review
16	Final Review
17	Final Review
18	Final Review
19	Final Review
20	Final Review
21	Final Review
22	Final Review
23	Final Review
24	Final Review
25	Final Review
26	Final Review
27	Final Review
28	Final Review
29	Final Review
30	Final Review
31	Final Review
32	Final Review
33	Final Review
34	Final Review
35	Final Review
36	Final Review
37	Final Review
38	Final Review
39	Final Review
40	Final Review
41	Final Review
42	Final Review
43	Final Review
44	Final Review
45	Final Review
46	Final Review
47	Final Review
48	Final Review
49	Final Review
50	Final Review
51	Final Review
52	Final Review
53	Final Review
54	Final Review
55	Final Review
56	Final Review
57	Final Review
58	Final Review
59	Final Review
60	Final Review
61	Final Review
62	Final Review
63	Final Review
64	Final Review
65	Final Review
66	Final Review
67	Final Review
68	Final Review
69	Final Review
70	Final Review
71	Final Review
72	Final Review
73	Final Review
74	Final Review
75	Final Review
76	Final Review
77	Final Review
78	Final Review
79	Final Review
80	Final Review
81	Final Review
82	Final Review
83	Final Review
84	Final Review
85	Final Review
86	Final Review
87	Final Review
88	Final Review
89	Final Review
90	Final Review
91	Final Review
92	Final Review
93	Final Review
94	Final Review
95	Final Review
96	Final Review
97	Final Review
98	Final Review
99	Final Review
100	Final Review

FOR THE COMMANDER: *John P. Huss*

Unclassified

SECURITY CLASSIFICATION OF THIS PAGE(When Data Entered)

20. (Cont)

input impedance. Additionally, bandwidth data and coupling data are also presented for both types of antennas.

Finally, the voltage breakdown levels for the J-slot, both air filled and dielectric filled, were determined.

Unclassified

SECURITY CLASSIFICATION OF THIS PAGE(When Data Entered)

Preface

The authors wish to thank all the other members of the branch who contributed their help without hesitation. They particularly want to thank Branch Chief Walter Rotman for overall guidance and Dr. J. L. Poirier for supervisory assistance.

Contents

1. INTRODUCTION	7
2. FLUSH MOUNTED ANNULAR SLOTS	8
3. J-SLOTS	21
4. CONCLUSIONS	30
REFERENCES	32

Illustrations

1. Cavity Backed, Dielectric Filled Slots Mounted in Base of Cone	9
2. Nose Cone Dimensions	9
3. Feed Network for Slot Antennas	10
4. Schematic of Pattern Range	10
5. Simulation of an Overdense Plasma by Metal Flares	11
6. Radiation Pattern: Flush Mounted Slots (2- and 4-in. In Flange)	13
7. Radiation Pattern: Flush Mounted Slots (2- and 4-in. Out Flange)	13
8. Radiation Pattern: Flush Mounted Slots (2- and 4-in. In and Out Flanges)	14
9. Radiation Pattern: Flush Mounted Slots vs Frequency (No Flange)	14

Illustrations

10.	Radiation Pattern: Flush Mounted Slots at 910 MHz (No Flange, 2- and 4-in., In and Out)	15
11.	Radiation Pattern: Flush Mounted Slots vs Frequency (4-in. In and Out Flange)	15
12.	Impedance of Rectangular Slot (Annular Slots Loaded, No Flanges)	17
13.	Impedance of Rectangular Slot vs Frequency (With In Flanges)	18
14.	Impedance of One Annular Slot vs Frequency (No Flanges)	19
15.	Impedance of Single Annular Slot vs Frequency (With In Flanges)	20
16.	Scale Model Metal Cone With J-Slots	21
17.	Radiation Pattern: J-Slots Fed Out of Phase (No Flange, 1- and 2-in. Out Flange)	23
18.	Radiation Pattern: J-Slots Fed Out of Phase (No Flange, 1-, 2-, and 4-in. In Flange)	23
19.	Radiation Pattern: J-Slots Fed Out of Phase (4-in. In and Out Flange)	24
20.	Radiation Pattern: J-Slots Fed in Phase (No Flange, 2- and 4-in. In Flange)	24
21.	Radiation Pattern: J-Slots Fed in Phase (No Flange, 2- and 4-in. Out Flange)	25
22.	Radiation Pattern: J-Slots Fed in Phase (4-in. In and Out Flange)	25
23.	Impedance of J-Slot vs Frequency (With/Without Flanges)	26
24.	Scale Model Metal Cone With J-Slots (For Breakdown Measurements)	27
25.	Voltage Breakdown vs Pressure for J-Slots (Air and Teflon Filled; $p_w = 1 \mu s$)	28
26.	Voltage Breakdown vs Pressure for J-Slots (Air and Teflon Filled; $p_w = .3 \mu s$)	28
27.	Voltage Breakdown vs Pressure for Air Filled Slot (Varying Pulse Widths)	29

Tables

1.	Annular Slot Coupling With Rectangular Slot Matched (Inward Flared Flanges)	12
2.	Annular Slot Coupling With Rectangular Slot Shorted (Inward Flared Flanges)	12
3.	Coupling Difference Between Annular Slots With Rectangular Slot Matched and Shorted	16
4.	Coupling Between Two J-Slots (Without Flanges)	27

Experimental Simulated Plasma Results on Base-Mounted Antennas

1. INTRODUCTION

The passage of reentry vehicles into the atmosphere, from the moment of actual reentry at some high altitude until mission accomplishment at a lower altitude, presents a multiplicity of problems. Some of these problems are unique to a specific mission; others, like plasma formation, are present for all reentry vehicles though in varying degrees of severity. Types of solutions to plasma problems are also varied, depending upon the particular reentry vehicle and its mission. For example, the Trailblazer II project^{1,2,3} attacked the problem of radio blackout caused by the formation of a plasma sheath around the reentry vehicle, thereby "blacking out" communications between ground and the vehicle. A two-fold investigation evolved: one phase dealt with actual flight experiments and the other phase with simulated plasma conditions in the laboratory.

(Received for publication 14 July 1976)

1. Hayes, D. T. et al (1972) Preliminary Report on the Trailblazer II Chemical Alleviation Flight of 28 July 1972, AFCRL-72-0640.
2. Lennon, J. F. (1973) Trailblazer II Rocket Tests on the Reentry Plasma Sheath: Vehicle Performance and Plasma Predictions Flights 1-3, AFCRL-TR-73-0317.
3. Karas, N. V. (1974) Laboratory and Flight Results of the Microstrip Plasma Probe, AFCRL-TR-74-0617.

Similarly the problems associated with the arming and fuzing of airborne vehicles under reentry environmental conditions can be attacked either by gathering data from flight experiments or from simulation of flight conditions. This report presents experimental laboratory data concerning the effects of a simulated plasma environment on patterns, impedance, and voltage breakdown levels of base-mounted antennas. The antenna configurations tested were: (1) flush mounted annular slots, and (2) J-slots.

2. FLUSH MOUNTED ANNULAR SLOTS

The descriptive designation of "windowless antennas" is applied to those antennas which exhibit the phenomena of radiating most of their energy in a direction opposite to that faced by the radiating aperture. One of such a group of antennas (consisting of two annular and one rectangular cavity-backed, dielectric-filled flush mounted slots) is shown in Figure 1. Investigation into pattern shape, bandwidth, impedance, and gain on similar shaped slots (though air filled) was conducted by General Electric.^{4,5} Figure 2 shows the cone dimensions in terms of the operating frequency and Figure 3 shows the feed circuit. This feed circuit was phased and the power divided between the antennas in such a way as to obtain nose-on coverage and an aft-on null. In the nomenclature of mode operation (in which an annular slot on an axisymmetric body can be excited by various azimuthal modes having field variations of the form $\cos n\theta$, or a combination) the antennas were operated in the $n = 1$ mode. Specifically, as shown in Figure 3, the source power was first evenly divided (power divider 1) with one arm feeding the linear slot and the other arm feeding another power divider (power divider 2) which in turn evenly split that power between the two annular slots. Variable phase and attenuation controls were inserted in the linear slot arm to adjust for maximum depth of null in the aft-on direction of the cone, and also, 180° phase shift was inserted between the arm feeding the two annular slots. All of the patterns (linear horizontal polarization) taken of this antenna grouping were principal E-plane cuts in which the nose cone itself was oriented axially parallel to the ground with the linear slot oriented vertical to the ground (see Figure 4).

4. Goldman, R. H. et al (1972) Windowless Antenna Design Study, General Electric Rpt., No. 72SDR2003, Reentry & Environmental Systems Div., Philadelphia, PA 19101.
5. Kinkead, W. K. and Sosin, W. L. (1976) Hardened Base Antenna Program Volume I, Air Force Rpt. No. SAMSO TR-76-61; GE Rpt. No. 76DR2055, Reentry & Environmental Systems Div., 3198 Chestnut St., Philadelphia, PA 19101.

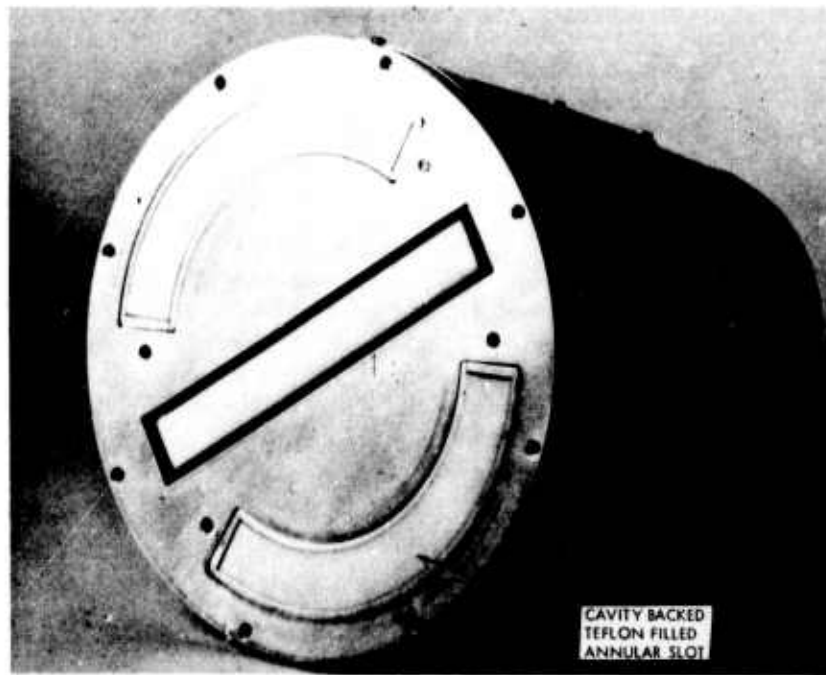


Figure 1. Cavity Backed, Dielectric Filled Slots Mounted in Base of Cone

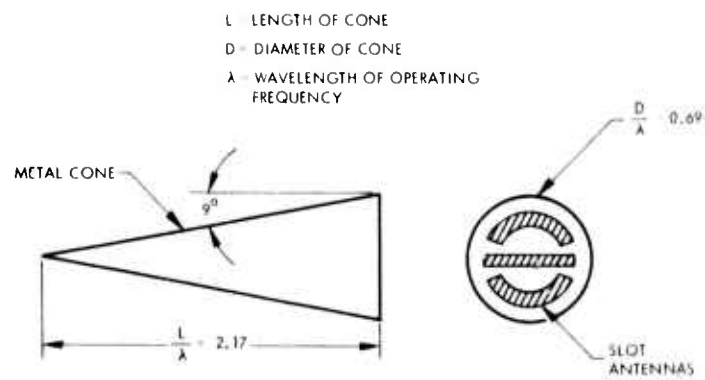


Figure 2. Nose Cone Dimensions

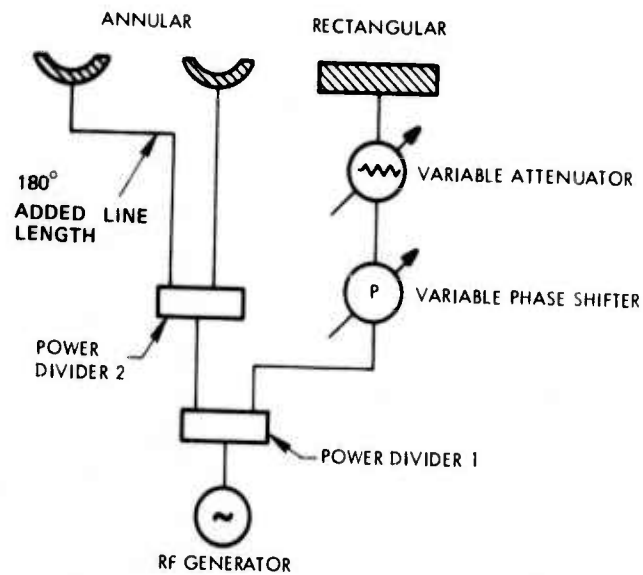


Figure 3. Feed Network for Slot Antennas

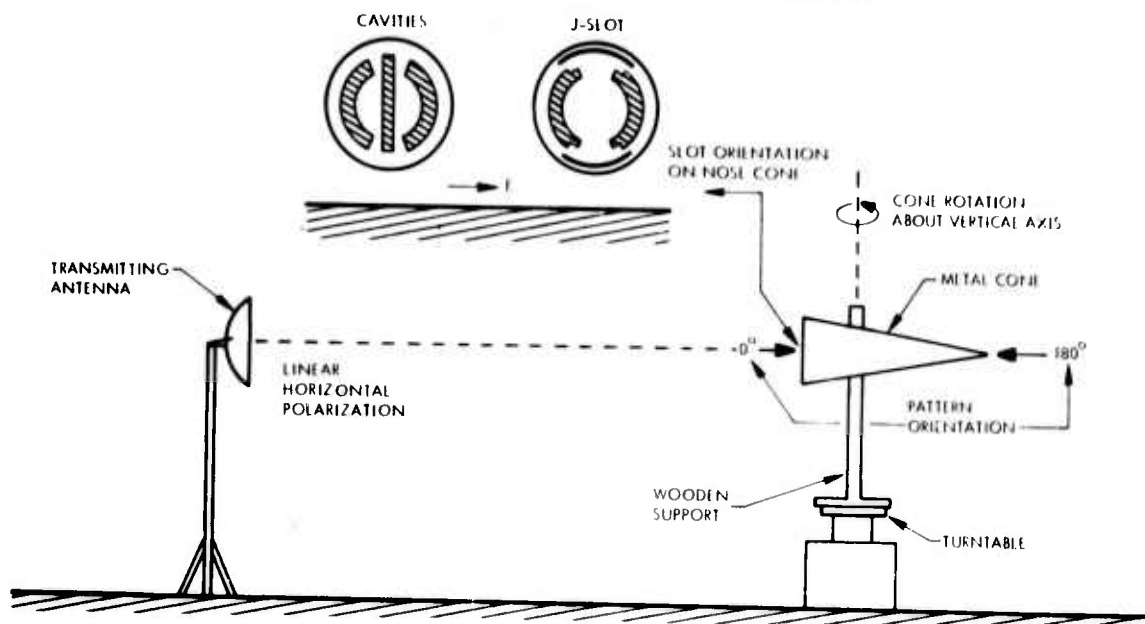


Figure 4. Schematic of Pattern Range

As stated in the introduction, reentry vehicles undergo severe environmental conditions and one consequence is the possible degradation of antenna performance at crucial periods of the flight thus causing failure of the mission. The problem of overcoming detrimental performance of vehicle antennas can be attacked either by studying the environmental effects during active flight experiments or simulating

the effects of some particular environmental aspect in the laboratory.⁶ All the data in this report stems from the experimental condition in which the radiating antennas were hooded by flared metal flanges (see Figure 5) which simulated an overdense plasma condition. The flared extensions (both inward and outward from the rim of the base of the cone) ranged in length from 1 to 4 in., however, only those results are shown in which significant changes occurred between different length flares. The first presentation of data will be concerned with the effect of metal flared flanges on the radiation pattern of the flush mounted slot antenna system. All the pattern levels shown in this section and the next have been normalized to the gain of a half-wave dipole radiating in free space.

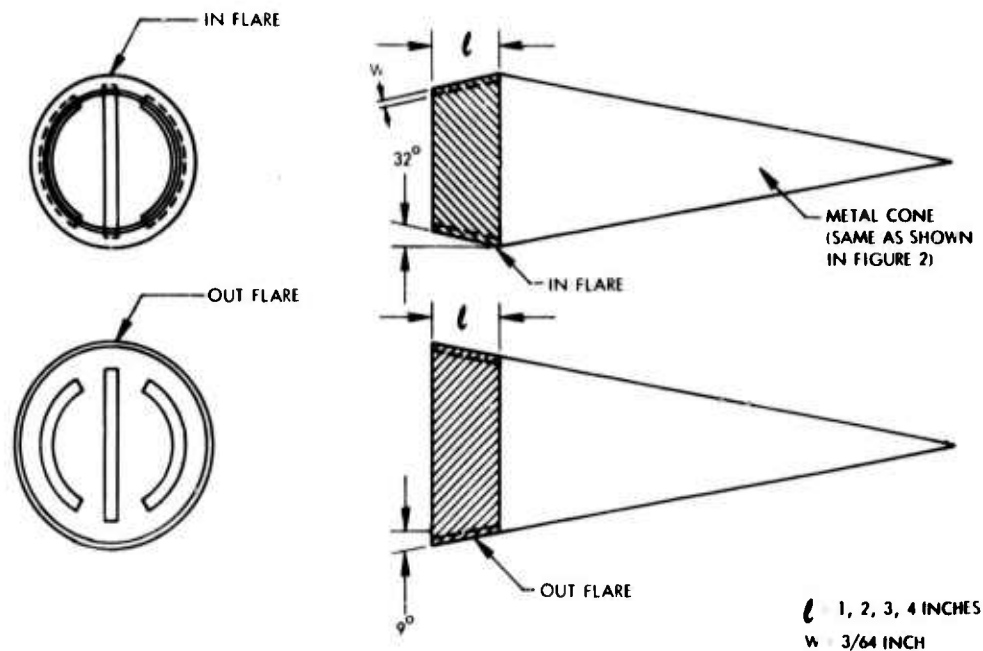


Figure 5. Simulation of an Overdense Plasma by Metal Flares

Figure 6 shows the effect of a 2- and 4-in. metal flange flared inward, and the antennas fed at the center frequency (for this measurement and all subsequent ones) of 900 MHz. The aft null fills when the 2-in. flange is added, the 4-in. flange only accentuates the rise in gain. The 1-in. flange had little effect. Somewhat similar results are obtained with the 2- and 4-in. flange flared outward, as shown in

6. Informal document (1974) Plasma Simulation Measurements on Reentry Vehicle Base Antennas, The Aerospace Corp., El Segundo, California (27 Mar 1974)

Figure 7. Next, Figure 8 combines, for easy visual comparison, the four patterns obtained by using the flanges. Though the flanges affect the gain in the aft-on direction differently, note that all have effectively filled in the null. To obtain a feeling for the bandwidth of this antenna system grouping, a frequency run is shown in Figure 9. The narrow band characteristics are evident by the rapid filling in of the null, though the frequency increased only by 5 MHz. Figure 10 illustrates that once the null has been filled in, for example by a shift in frequency from the center frequency, then addition of the flanges only moderately affects the shape of the patterns. Finally, Figure 11 shows the marginal effects of a frequency shift once the flanges have filled in the null. Conversely, once a frequency shift has destabilized the pattern, further changes due to environmental conditions are minimal. Effectively the null has been destroyed whether it be from a frequency shift or a plasma condition.

Coupling measurements were made between the two annular slots. For the data shown in Table 1 the rectangular slot output was terminated by a matched load.

Table 1. Annular Slot Coupling With Rectangular Slot Matched (Inward Flared Flanges)

Frequency (MHz)	COUPLING (-db)		
	No Flange	2-in. Flange	4-in. Flange
920	22.6	16.2	13.2
910	18.8	13.0	10.5
900	14.8	9.5	6.5
890	13.0	7.0	4.0
880	13.6	7.0	3.0

For the data shown in Table 2, the rectangular slot was covered by metal foil.

Table 2. Annular Slot Coupling With Rectangular Slot Shorted (Inward Flared Flanges)

Frequency (MHz)	COUPLING (-dB)		
	No Flange	2-in. Flange	4-in Flange
920	15.0	10.5	8.8
910	14.0	8.8	6.9
900	13.0	7.3	5.2
890	13.0	6.5	-
880	14.3	6.5	-

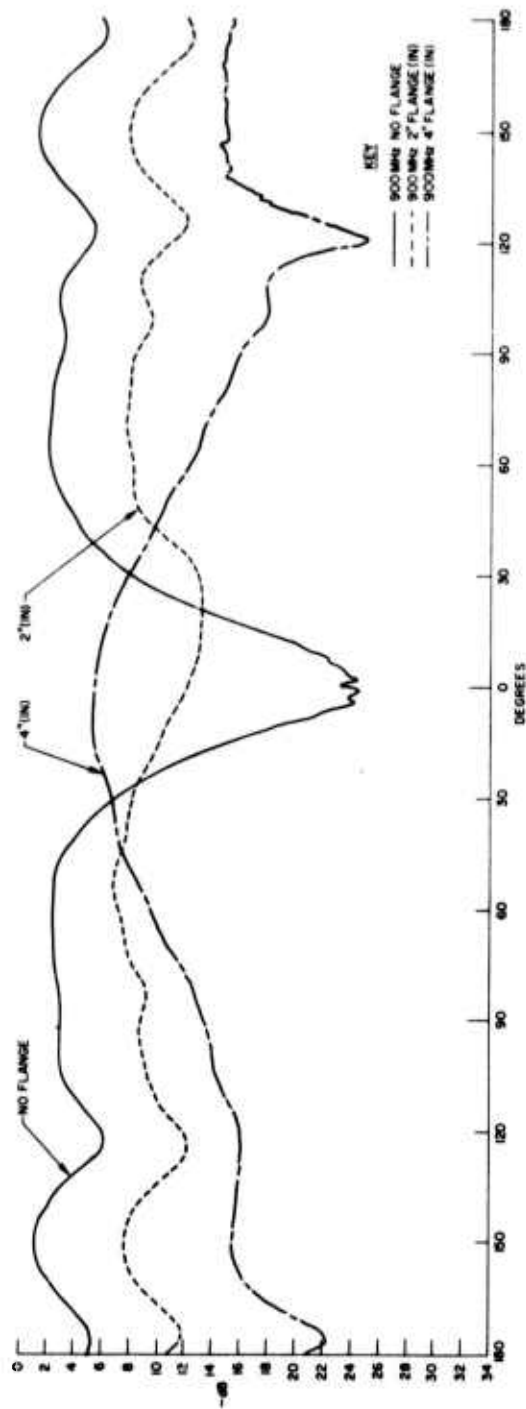


Figure 6. Radiation Pattern: Flush Mounted Slots (2- and 4-in. In Flange)

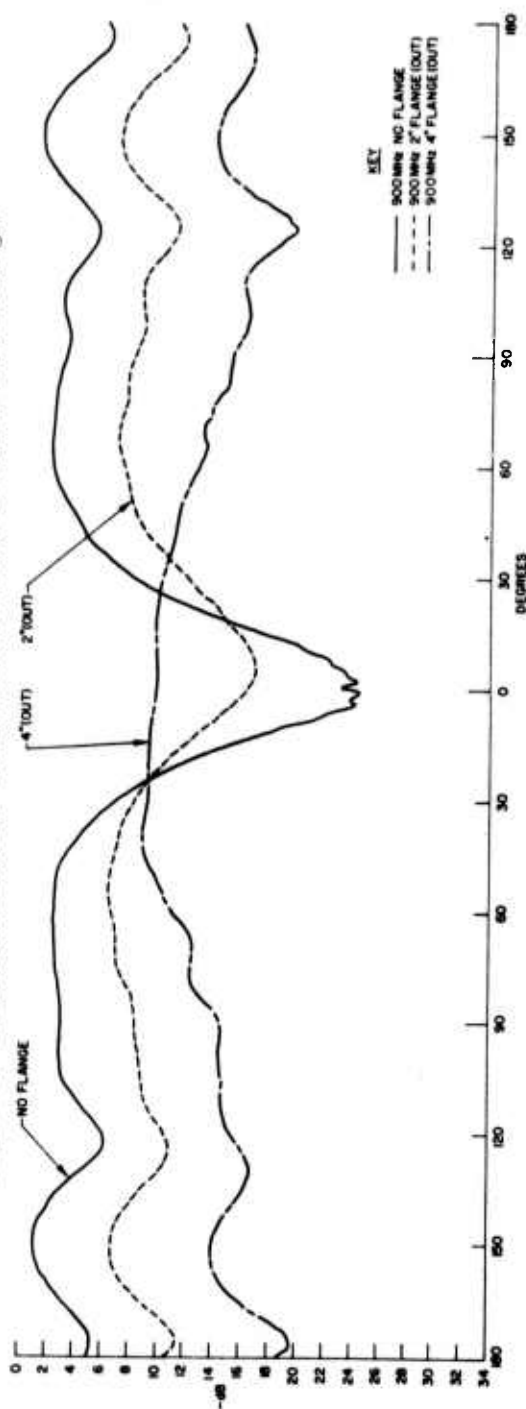


Figure 7. Radiation Pattern: Flush Mounted Slots (2- and 4-in. Out Flange)

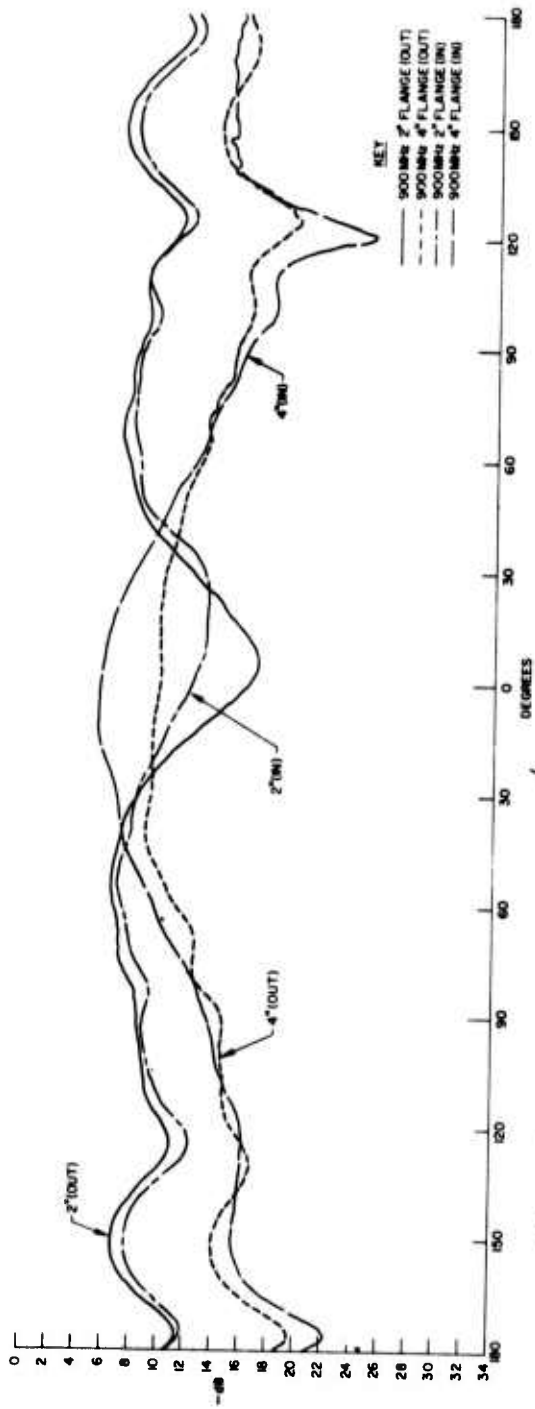


Figure 8. Radiation Pattern: Flush Mounted Slots (2- and 4-in. In and Out Flanges)

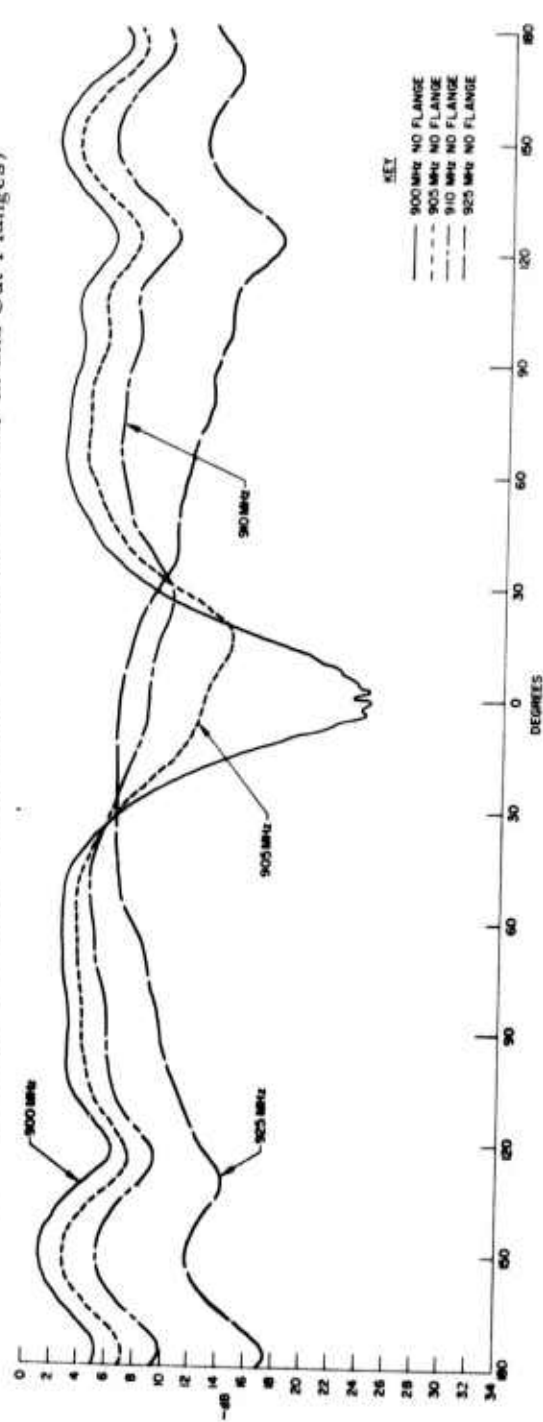


Figure 9. Radiation Pattern: Flush Mounted Slots vs Frequency (No Flange)

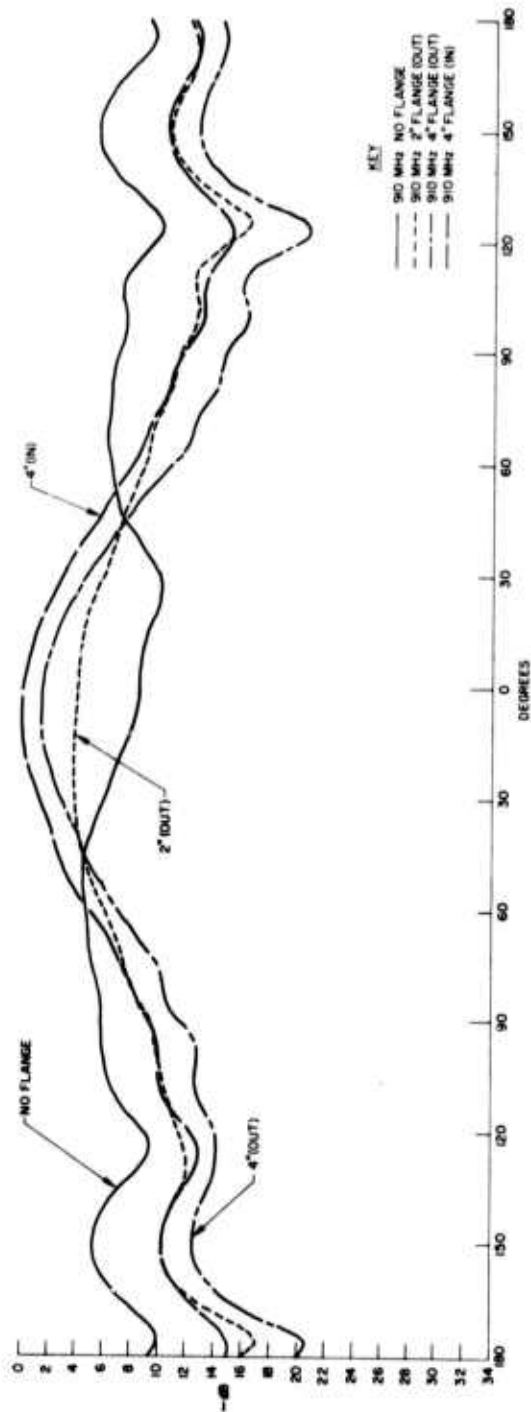


Figure 10. Radiation Pattern: Flush Mounted Slots at 910 MHz (No Flange, 2- and 4-in., In and Out)

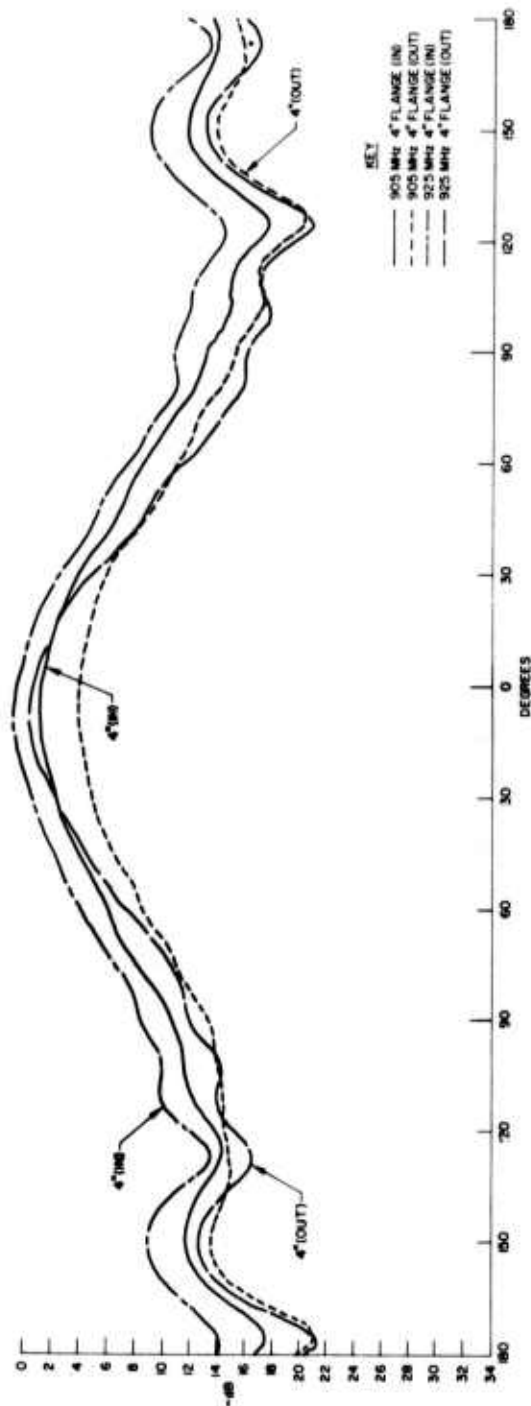


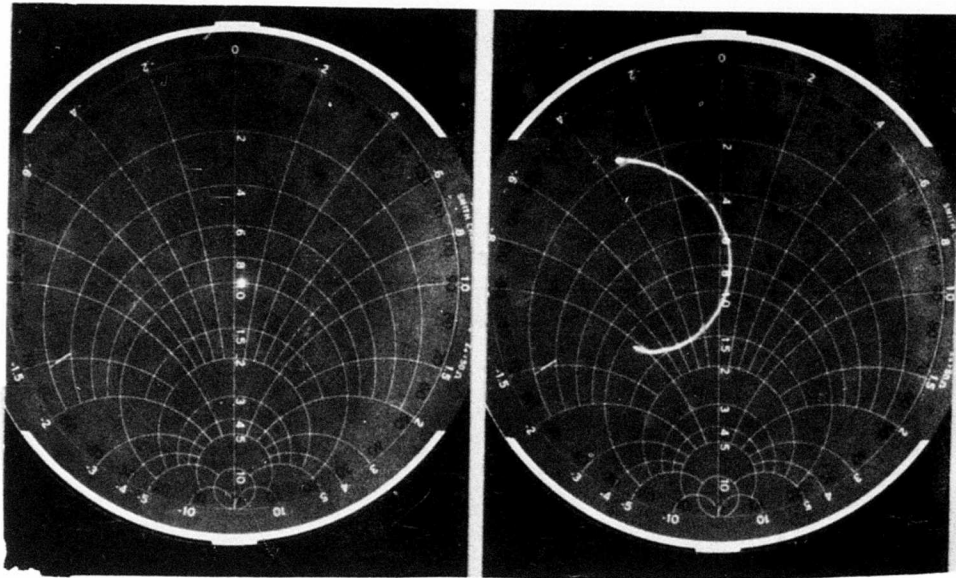
Figure 11. Radiation Pattern: Flush Mounted Slots vs Frequency (4-in., In and Out Flange)

Table 3 shows the difference in coupling between the annular slots when the rectangular slot is present and when it is shorted (effectively removed).

Table 3. Coupling Difference Between Annular Slots, With the Rectangular Slot Matched and Shorted

Frequency (MHz)	COUPLING DIFFERENCE (± dB from Shorted Rectangular Aperture)		
	No Flange	2-in. Flange	4-in. Flange
920	+7.6	+5.7	+4.4
910	+4.8	+4.2	+3.6
900	+1.8	+2.2	+1.3
890	0.0	+0.5	-
880	-0.7	+0.5	-

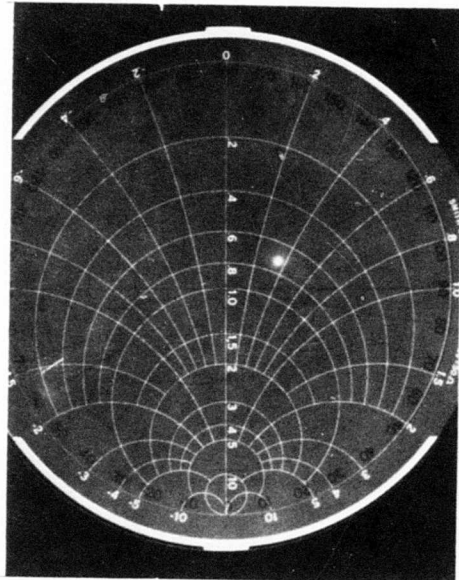
The final set of data concerning these flush mounted slots are Smith chart presentations of impedance, as shown in Figures 12, 13, 14 and 15. The lower frequency location can be identified by the bright dot on the upper end of the impedance arc. The first two of these figures shows the impedance vs frequency for the rectangular with the two annular slots terminated in matched loads. The reactance, for off center frequencies, is predominantly capacitive. The third figure (Figure 14) shows the impedance of one annular slot, with the other annular and the rectangular terminated in matched loads and the fourth figure of this series shows the effect of the 2- and 4-in. in-flanges on the impedance.



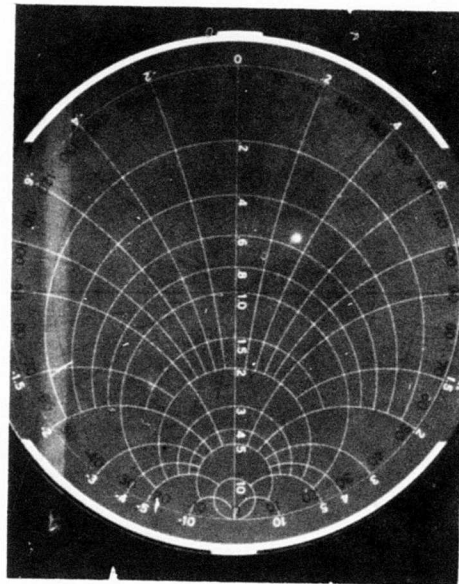
900 MHz (No Flange)

875 - 925 MHz (No Flange)

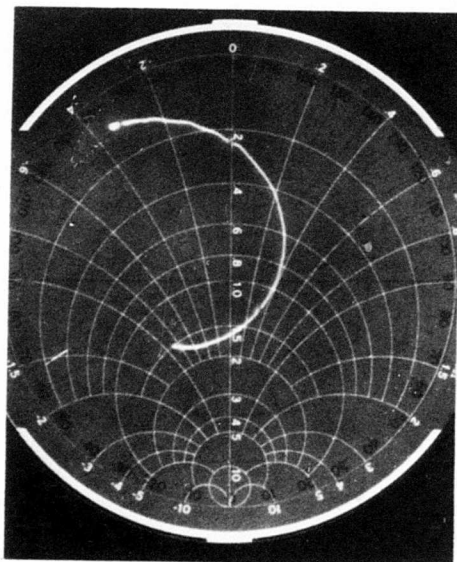
Figure 12. Impedance of Rectangular Slot (Annular Slots Loaded, No Flanges)



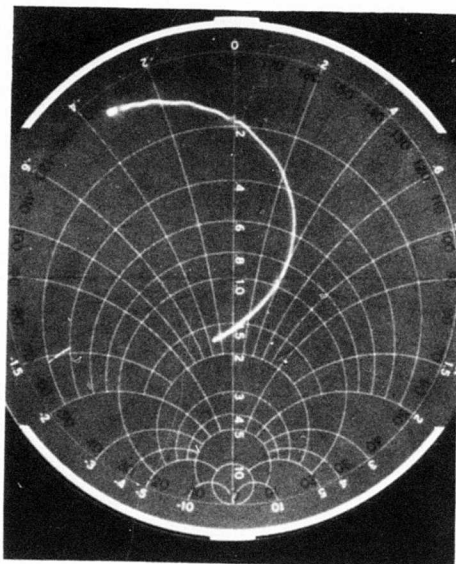
900 MHz (2 - In. Flange)



900 MHz (4 - In. Flange)

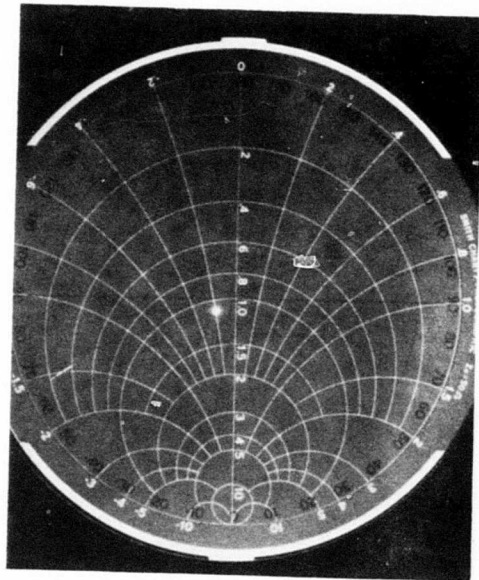


875 - 925 MHz (2-In. Flange)

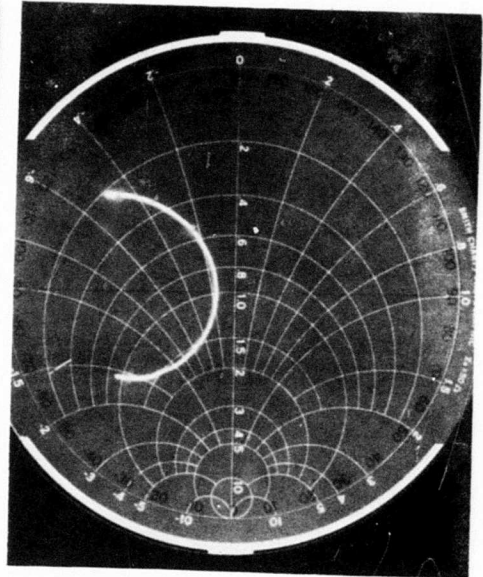


875 - 925 MHz (4-In. Flange)

Figure 13. Impedance of Rectangular Slot vs Frequency (With In Flanges)



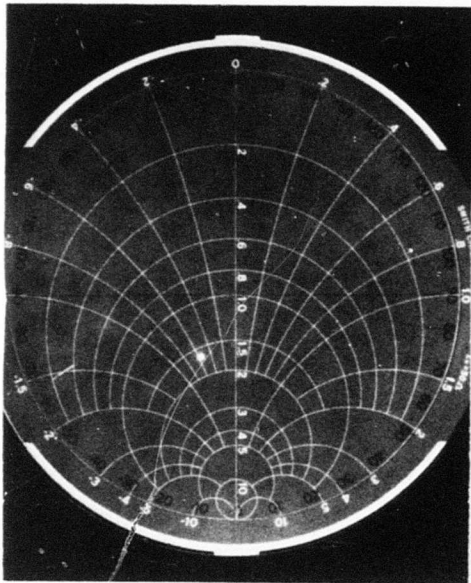
900 MHz (No Flange)



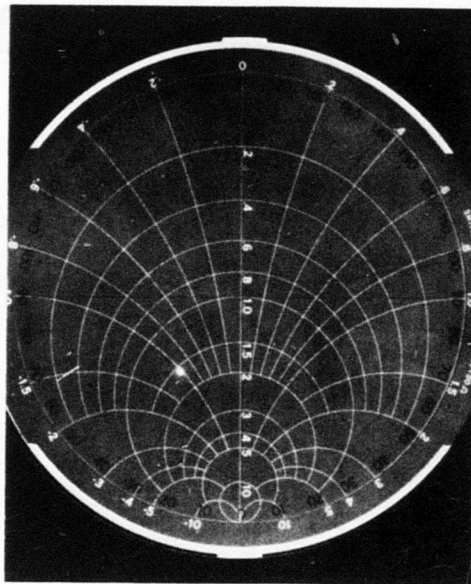
875 - 925 MHz (No Flange)

(Other Annular Slot and Rectangular Slot Loaded)

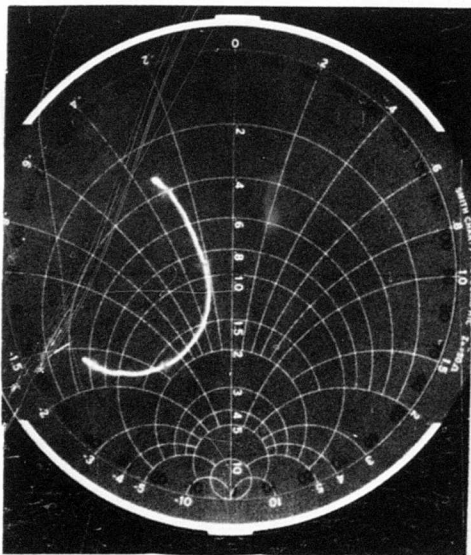
Figure 14. Impedance of One Annular Slot vs Frequency (No Flanges)



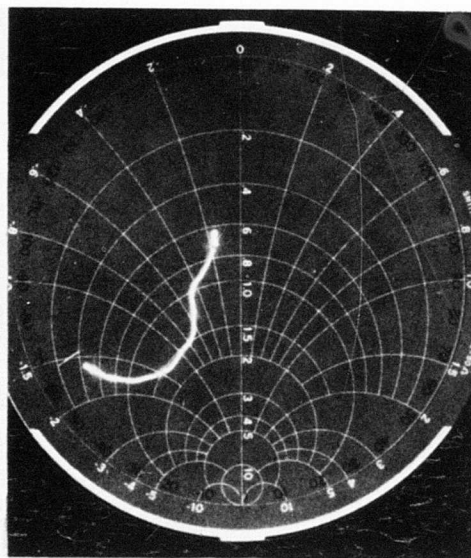
900 MHz (2 In. Flange)



900 MHz (4 - In. Flange)



875 - 925 MHz (2 - In. Flange)



875 - 925 MHz (4 - In. Flange)

Figure 15. Impedance of Single Annular Slot vs Frequency (With In Flanges)

3. J-SLOTS

In the search for not only suitable antennas which can be base-mounted but also for those shapes that can be more usefully utilized in the accomplishment of a mission, many designs have been proposed and tested (that is, multiple stubs, slot and stub array, single stubs, and annular slots [see also Reference 6]). Among the more useful type are those designated as J-slots.

Figure 16 shows a scale model cone and the two J-slots that were used in the first phase of the experiment: gathering data on pattern, impedance, and coupling changes due to simulated plasma conditions. The cone size was the same as that shown in Figure 2, the operating center frequency was 900 MHz and patterns were taken with the two J-slots oriented for linear horizontal polarization (see Figure 4). The J-slots can be operated in two modes. For the first mode, with nulls at 0° and 180° and maximum broadside radiation, the two antennas are fed in phase. For the second mode, with a null in the aft-on position and maximum radiation nose-on, the two antennas are fed 180° out of phase.

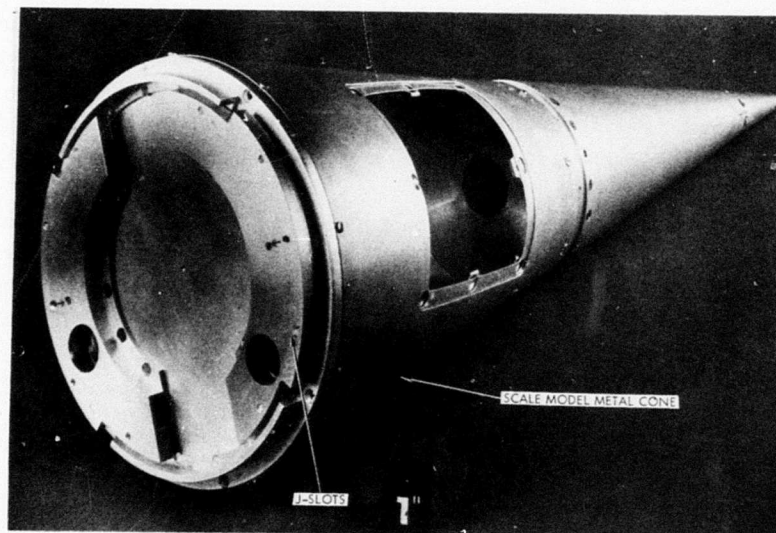


Figure 16. Scale Model Metal Cone With J-Slots

Figures 17, 18 and 19 are of the antennas fed out of phase. As in the flush mounted slots of the previous section all the power levels are relative to the gain of a dipole radiating in free space. Note in Figure 17 that the 1-in. flange drastically fills in the null, and that the 2-in. flange further raises the aft-on gain. Thereafter the 3-in. and 4-in. flanges have only a slight effect. Figure 18 shows similar results, the filling in of the aft-on null as in the previous figure, even though the antennas were hooded by the inward flared rather than the outward flared flange. Figure 19 shows this similarity of effect by the flared flanges. The next three figures depict the antennas fed in phase. In Figure 20 the null has been filled in approximately 10 dB by the 2 in. -flange, the gain has dropped between 5 to 7 dB, the half power beamwidth (measured from the peak humps on either side of 0°) has widened considerably, but the null position has barely shifted. The 4 in. -flange reduces the gain by approximately 15 dB, and the null moves a few more degrees from the dead on null at 0° . The outward flared flanges have moderately less effect on the overall pattern than the inward flared, as shown in Figures 21 and 22. Also, the drop in overall gain and null filling is less. Figure 22 depicts these different flange effects more clearly.

As can be deduced from the design of the J-slots, a plasma buildup around the rim of the cone base significantly affects the antenna characteristics. Figure 23 contains the impedance of one J-slot, as a function of frequency, with and without a flange. Note that the 2 in. -flange seriously detunes the antenna.

The coupling data between two J-slots (without flanges) as a function of frequency is given in Table 4. The coupling remains relatively constant within the range of the frequency run.

In addition to the plasma simulation explorations, breakdown experiments in a belljar were conducted on a somewhat similar model which, however, was scaled to an operating frequency (for the J-slots) of approximately 1200 MHz. This second cone model (built under contract)⁷ had a base diameter of 6 in. (see Figure 24) though the cone angle remained at 9° .

7. Haldeman, C.W. et al (1975) Comparative Effects of Simulated Reentry Wake Plasma on Three Base - Mounted Microwave Antennas, AFCRL-TR-76-0013, Aerophysics Laboratory, Massachusetts Institute of Technology, Cambridge, Massachusetts 02139.

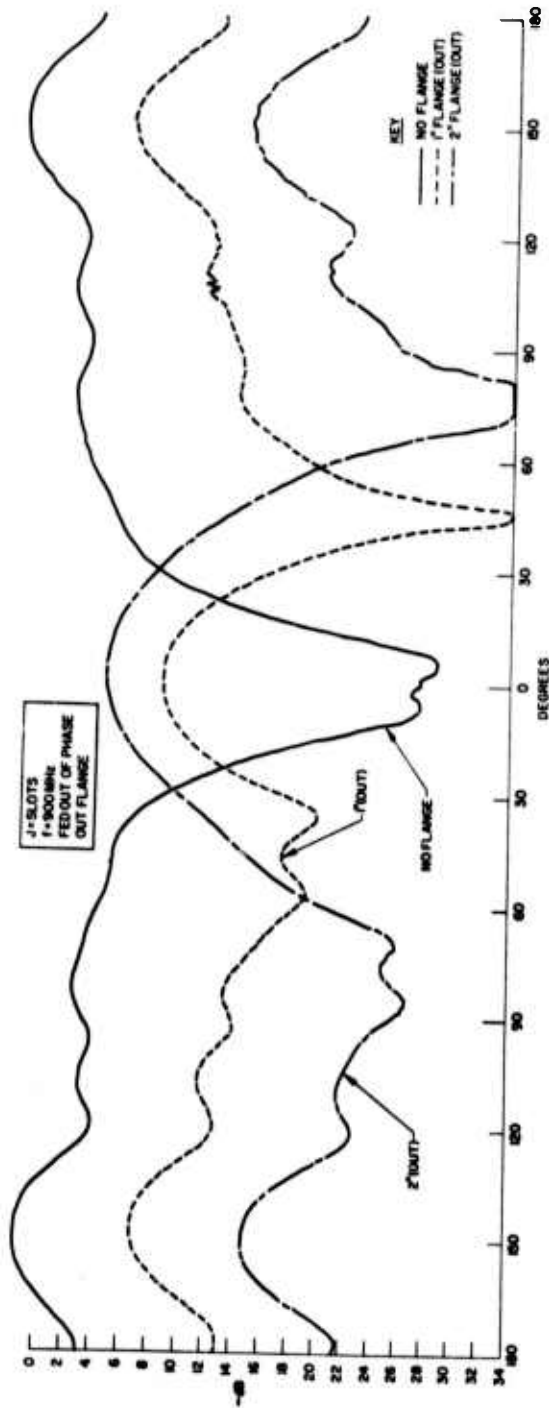


Figure 17. Radiation Pattern: J-Slots Fed Out of Phase (No Flange, 1- and 2-in. Out Flange)

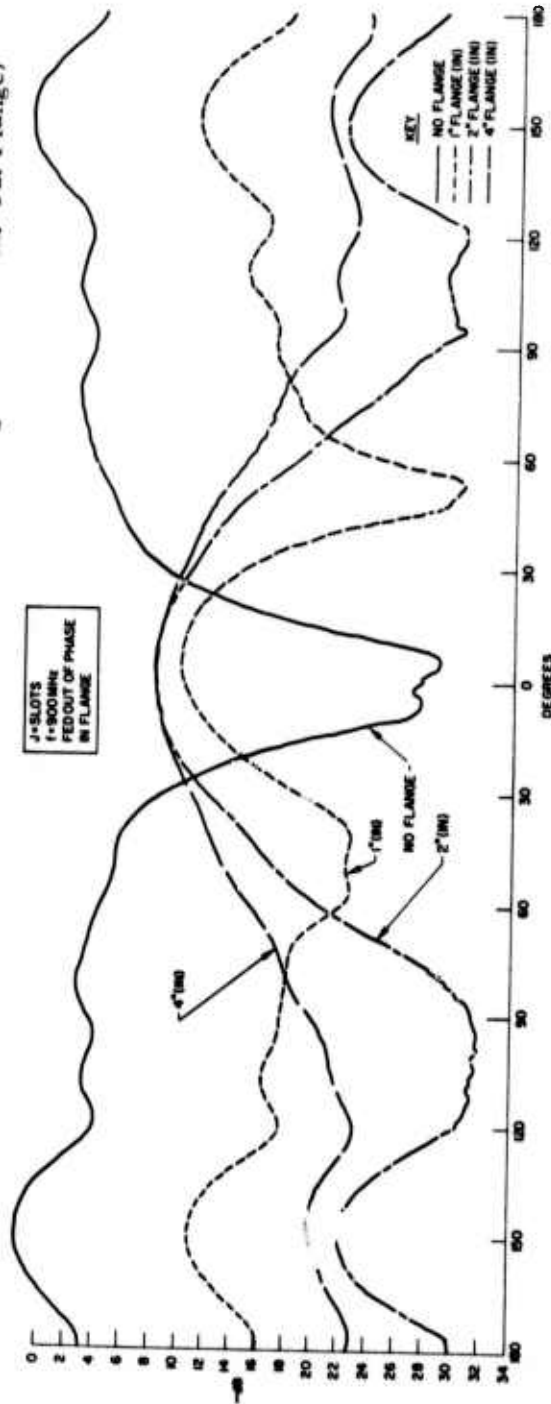


Figure 18. Radiation Pattern: J-Slots Fed Out of Phase (No Flange, 1-, 2-, and 4-in. In Flange)

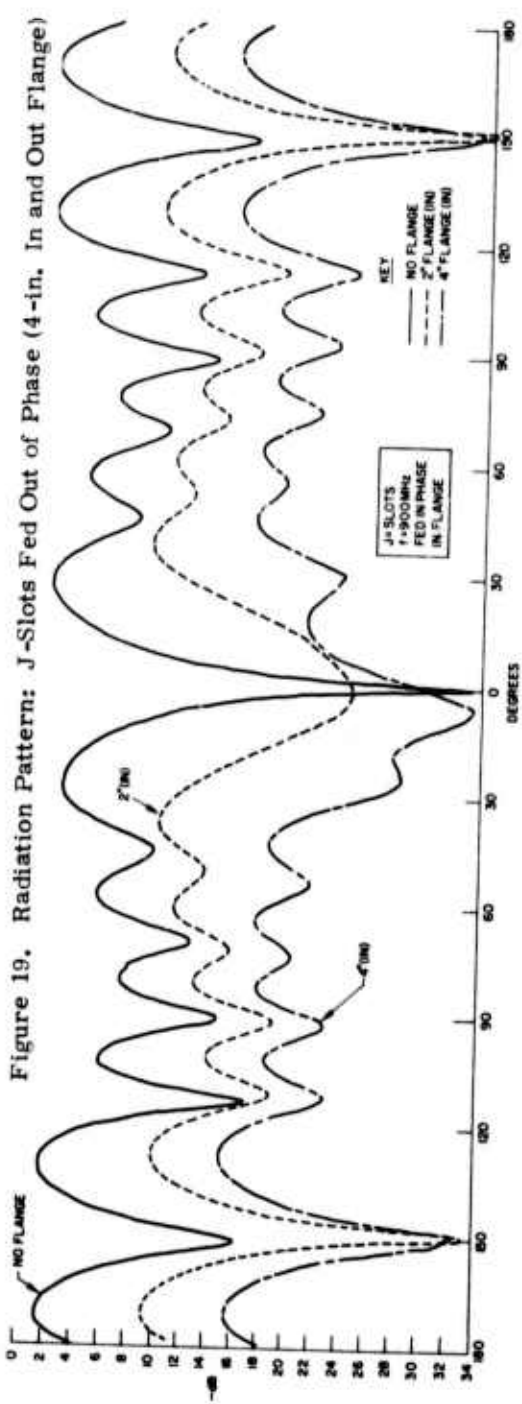
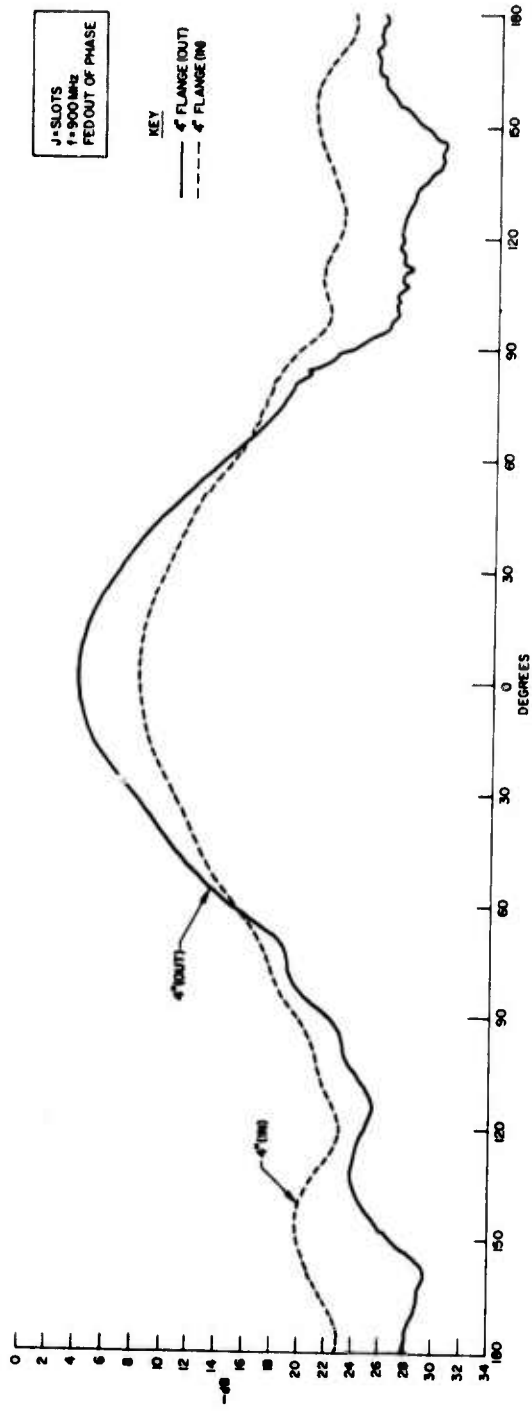


Figure 19. Radiation Pattern: J-Slots Fed Out of Phase (4-in. In and Out Flange)

Figure 20. Radiation Pattern: J-Slots Fed in Phase (No Flange, 2- and 2-in. In Flange)

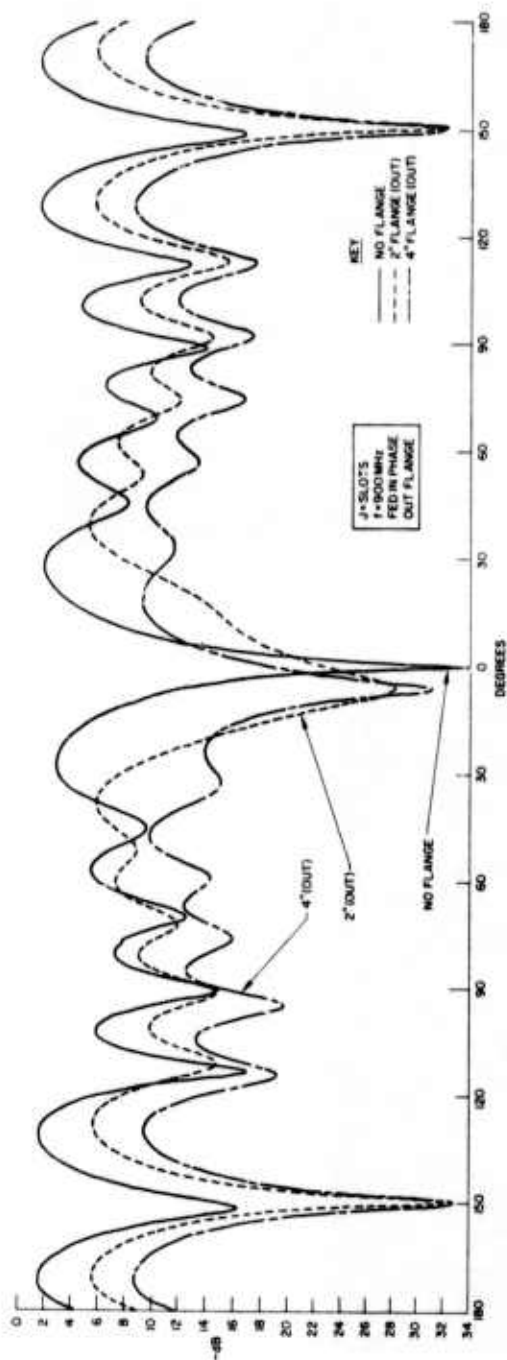


Figure 21. Radiation Pattern: J-Slots Fed in Phase (No Flange, 2- and 4-in. Out Flange)

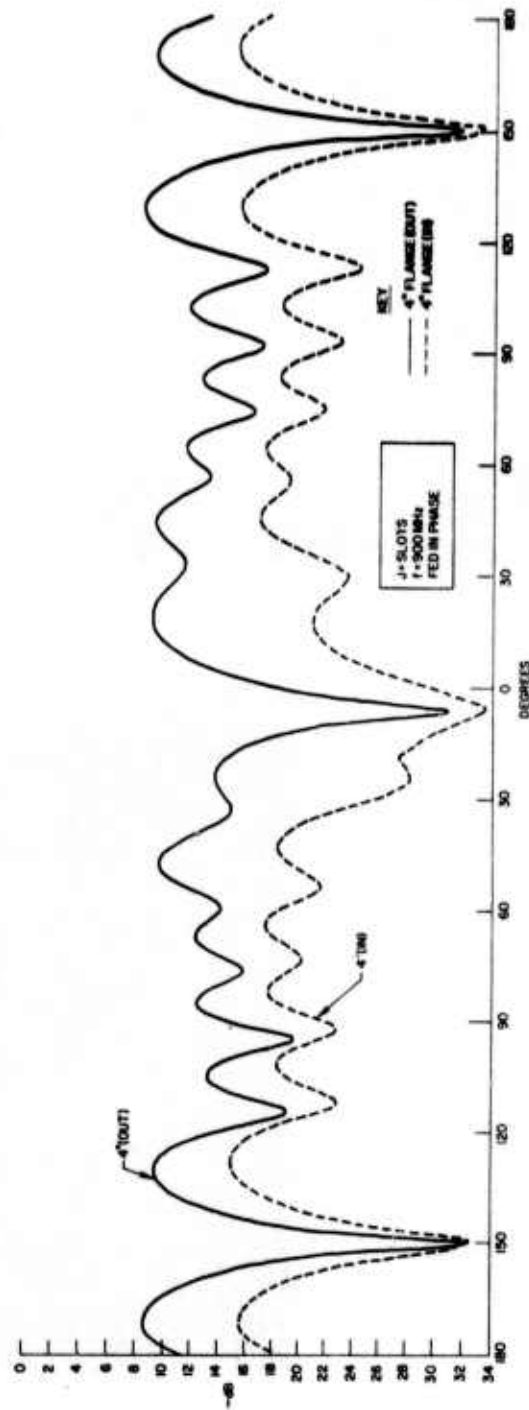
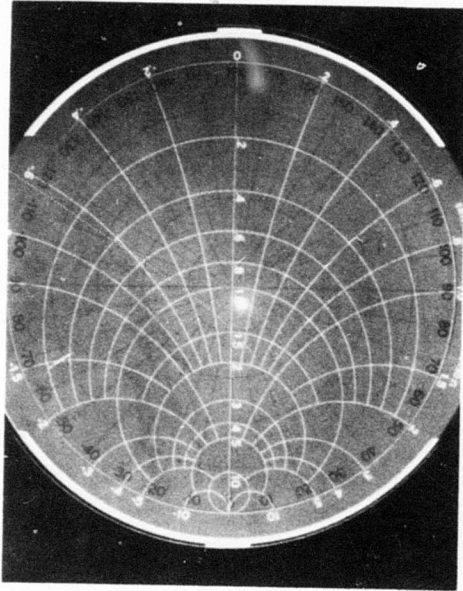
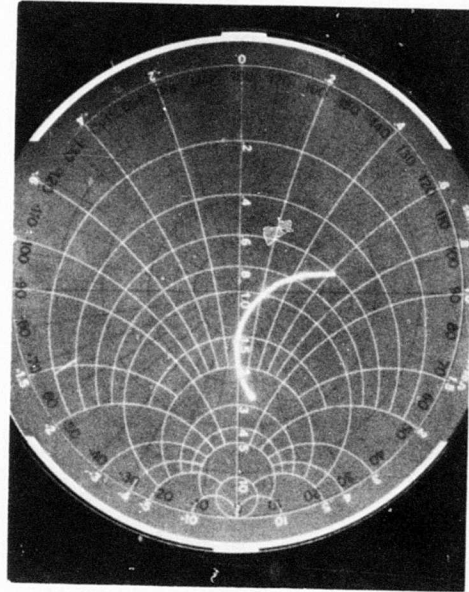


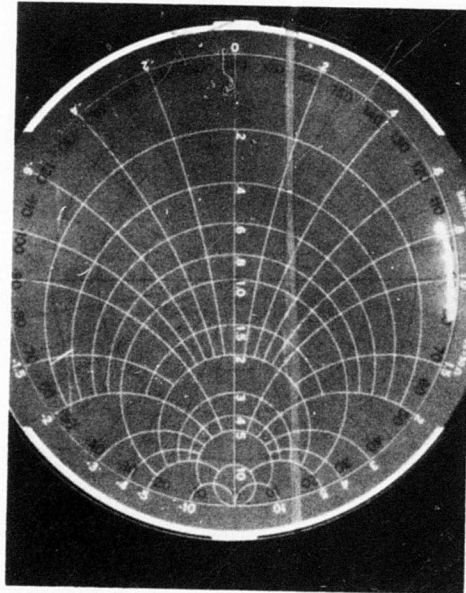
Figure 22. Radiation Pattern: J-Slots Fed in Phase (4-in. In and Out Flange)



900 MHz (No Flange)



875 - 925 MHz (No Flange)



875 - 925 MHz (2 - In. Flange)

Figure 23. Impedance of J-Slot vs Frequency (With/Without Flanges)

Table 4. Coupling Between Two J-Slots (Without Flanges)

Frequency (MHz)	Coupling (-dB)
920	20.2
910	20.3
900	20.8
890	21.5
880	22.0

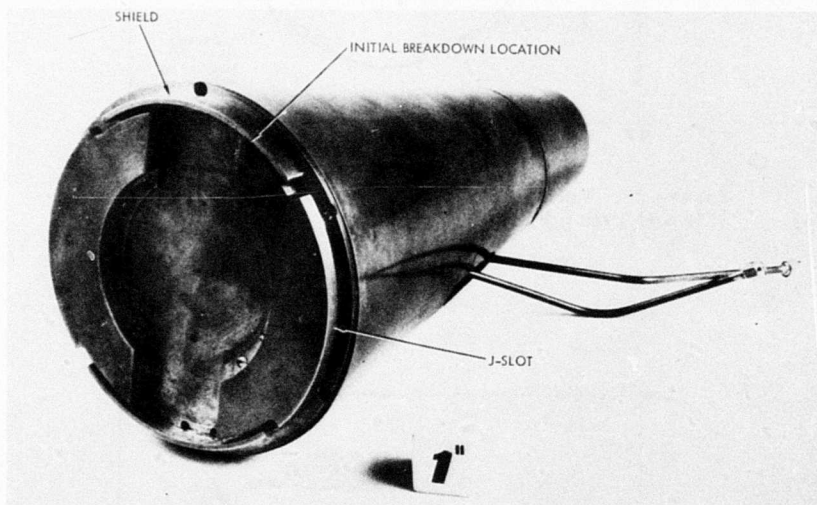


Figure 24. Scale Model Metal Cone With J-Slots (For Breakdown Measurements)

Figure 25 compares the voltage breakdown levels for air and teflon filled J-slots (pulse width $1 \mu s$, pulse period 10^{-3} sec). Minimum breakdown voltage for the air-filled slot occurred at about 25 W peak; increasing to about 35 W peak for the teflon-filled slot. Filling the gap with dielectric detuned the antenna and in order to retune it, the gap was widened and the operating frequency lowered. Figure 26 compares minimum breakdown levels of the same model but the pulse width has been narrowed to $0.3 \mu s$. Again, for the air-filled gap, the minimum voltage breakdown level is approximately 25 W; for the teflon-filled gap the voltage rises to about 40 W. The effects of different pulse widths on breakdown levels is shown in Figure 27 (no change in breakdown level occurred).

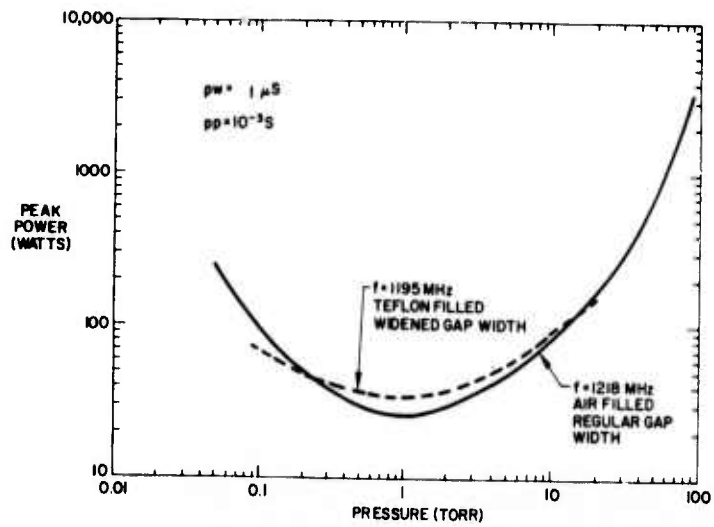


Figure 25. Voltage Breakdown vs Pressure for J-Slots (Air and Teflon Filled; $p_w = 1 \mu s$)

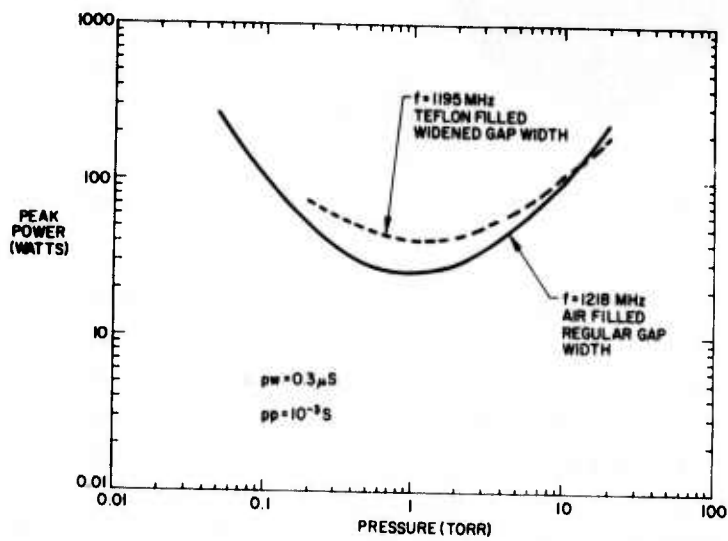


Figure 26. Voltage Breakdown vs Pressure for J-Slots (Air and Teflon Filled $p_w = 0.3 \mu s$)

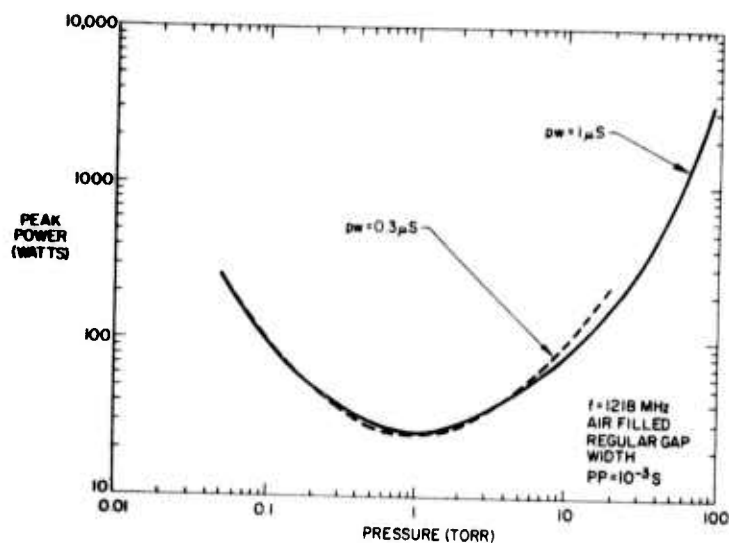


Figure 27. Voltage Breakdown vs Pressure for Air Filled Slot (Varying Pulse Widths)

For convenience, the teflon inserts were individual pieces instead of a single, precision machined piece. Therefore, it is reasonable to assume that the minimum breakdown voltage level could be increased if the J-slot air spaces were filled with a milled insert. Breakdown initially occurred at the corners between the shield and the edge of the J-slot (see Figure 24).

Interpretation of these results⁸ for full scale antennas requires scaling of the results to other frequencies, and also estimating the gas density (which determines antenna breakdown rather than pressure) in the base region. By estimation, the gas density in the base region is approximately one-tenth the ambient value and the gas temperature low enough so that cold air measurements should suffice. However, even though the assumption is made that the ionization rates are not changing significantly, the possible presence of plasma from the expanding flow fields should be taken into account by a safety factor or by more tests.

For a given antenna design, a plot of power breakdown threshold vs the ratio of gas density to frequency should be invariant with frequency.⁹ Assuming a scale factor of three, the abscissa (pressure) of the graphs would have to be decreased by this factor to apply to the full scale antenna while the ordinate (power) remains unchanged. Consider a test case and assume an altitude of 50,000 ft (corresponding

8. Rotman, W. (1976) Private communication dated 8 Jan 1976.

9. Taylor, W.C. et al (1971) Voltage breakdown of microwave antennas, Advances in Microwaves, 17:Figure 9.

ambient pressure = 90 torr). For a full-sized antenna the equivalent base pressure is nine torr. Using a factor of three for a corresponding model pressure of 27 torr for the breakdown curve (air filled gap) in Figure 25, the power breakdown threshold is 250 W peak. If an additional factor (that is, 5) is applied to account for plasma effects and as a safety margin the final result for an operational system is about 50 W peak.

4. CONCLUSIONS

A plasma buildup around the base of reentry vehicles, which contain base mounted antennas as part of their electromagnetic radiation system, can seriously affect the performance of those antennas by drastically altering their electrical characteristics.

One deleterious plasma effect is the changing of pattern shape such that the implementation of the vehicle mechanism in order to accomplish the mission becomes difficult or, worse, impossible.

This pattern shape change (caused by a simulated overdense plasma) is shown in the figures and occurred both for the flush mounted cavity slots and also the protruding J-slots. Significant filling in of the null took place even when the simulated plasma extended outward from the base rim of the cone for a distance which was a small fraction of the operating wavelength. For example, with the cavities (see Figure 6) when the metal hood extended outward a distance of 0.15 wavelengths, the null filled in about 10 dB. When the hood was further extended to 0.30 wavelengths the null level rose approximately 18 dB above the null depth without the metal flange. Also the figures illustrate the narrow band characteristics of the cavity slots. From Figure 9, it is seen that a frequency change of less than 1 percent causes the null level to rise by about 10 dB. In addition to the change in the radiation patterns, the impedance characteristics also change, as can be seen from the Smith chart plots. One inevitable consequence of this impedance mismatch in the system is the drop of transmitted power.

If the simulated overdense plasma is present, the radiation patterns of the J-slots (fed out of phase) change more radically than do the radiation patterns of the cavity antennas. Figure 17 shows that the 1 in. -flange causes the null to fill in by about 18 dB and Figure 18 shows that the 2 in. -flange peaks the rise in the null. As can be seen from the figures the direction of the original pattern shapes reverse; the aft-on null peaking, the nose-on level dropping.

When the J-slots are fed in phase, the effect of the simulated plasma is subdued. The larger effect occurs with the inward flared flanges as can be seen by comparing the patterns in Figures 20 and 21. Both flange configurations move the

null by a few degrees from the dead-on position. However, the "in" flange (2 in.) fills in the null by about 10 dB whereas the "out" flange fills it in by only 5 dB. An anomalous behavior is shown in Figure 20, in that the 4 in. - flange lowers the null again. Figure 23 shows the drastic effect of the 2 in. - flange in the input impedance of one J-slot.

Initial voltage breakdown occurs between the end edge of the J-slot and the metal shield. This breakdown level can be raised by filling the J-slot with dielectric or widening the shield gap.

References

1. Hayes, D. T. et al (1972) Preliminary Report on the Trailblazer II Chemical Alleviation Flight of 28 July 1972, AFCRL-72-0640.
2. Lennon, J. F. (1973) Trailblazer II Rocket Tests on the Reentry Plasma Sheath: Vehicle Performance and Plasma Predictions Flights 1-3, AFCRL-TR-73-0317.
3. Karas, N. V. (1974) Laboratory and Flight Results of the Microstrip Plasma Probe, AFCRL-TR-74-0617.
4. Goldman, R. H. et al (1972) Windowless Antenna Design Study, General Electric Rpt., No. 72SDR2003, Reentry & Environmental Systems Div., Philadelphia, PA 19101.
5. Kinkead, W. K. and Sosin, W. L. (1976) Hardened Base Antenna Program Volume I, Air Force Rpt. No. SAMSO-TR-76-61, GE Rpt. No. 76DR2055, Reentry & Environmental Systems Div., 3198 Chestnut St., Philadelphia, PA 19101.
6. Informal document (1974) Plasma Simulation Measurements on Reentry Vehicle Base Antennas, The Aerospace Corp., El Segundo, California (27 Mar 1974).
7. Haldeman, C. W. et al (1975) Comparative Effects of Simulated Reentry Wake Plasma on Three Base - Mounted Microwave Antennas, AFCRL-TR-76-0013, Aerophysics Laboratory, Massachusetts Institute of Technology, Cambridge, Massachusetts 02139.
8. Rotman, W. (1976) Private communication dated 8 Jan 1976.
9. Taylor, W. C. et al (1971) Voltage breakdown of microwave antennas, Advances in Microwaves, 17:Figure 9.

MISSION
of
Rome Air Development Center

RADC plans and conducts research, exploratory and advanced development programs in command, control, and communications (C³) activities, and in the C³ areas of information sciences and intelligence. The principal technical mission areas are communications, electromagnetic guidance and control, surveillance of ground and aerospace objects, intelligence data collection and handling, information system technology, ionospheric propagation, solid state sciences, microwave physics and electronic reliability, maintainability and compatibility.



**Printed by
United States Air Force
Hanscom AFB, Mass. 01731**